

RESEARCH ARTICLE

# Preparation and optimization of doxorubicin-loaded albumin nanoparticles using response surface methodology

Lei Li<sup>1</sup>, Xiuli Zhao<sup>1</sup>, Chunrong Yang<sup>1,2</sup>, Haiyang Hu<sup>1</sup>, Mingxi Qiao<sup>1</sup>, and Dawei Chen<sup>1</sup>

<sup>1</sup>School of Pharmacy, Shenyang Pharmaceutical University, Shenyang, P. R. China and <sup>2</sup>College of Pharmacy, Jiamusi University, Jiamusi, P. R. China

## Abstract

**Background:** The objective of this work was to optimize the preparation of doxorubicin-loaded albumin nanoparticles (Dox-A-Nps) through desolvation procedures using response surface methodology (RSM). A central composite design (CCD) for four factors at five levels was used in this study.

**Method:** Albumin nanoparticles were prepared through a desolvation method and were optimized in the aid of CCD. Albumin concentration, amount of doxorubicin, pH values, and percentage of glutaraldehyde were selected as independent variables, particle size, zeta potential, drug loading, encapsulation efficiency, and nanoparticles yield were chosen as response variables. RSM and multiple response optimizations utilizing a quadratic polynomial equation were used to obtain an optimal formulation.

**Results:** The optimal formulation for Dox-A-Nps was composed of albumin concentration of 17 mg/ml, amount of doxorubicin of 2 mg/ml, pH value is 9 and percentage of glutaraldehyde of 125% of the theoretic amount, under which the optimized conditions gave rise to the actual average value of mean particle size ( $151 \pm 0.43$  nm), zeta potential ( $-18.8 \pm 0.21$  mV), drug loading efficiency ( $21.4 \pm 0.70\%$ ), drug entrapment efficiency ( $76.9 \pm 0.21\%$ ) and nanoparticles yield ( $82.0 \pm 0.34\%$ ). The storage stability experiments proved that Dox-A-Nps stable in 4°C over the period of 4 months. The *in vitro* experiments showed a burst release at the initial stage and followed by a prolonged release of Dox from albumin nanoparticles up to 60 h.

**Conclusions:** This study showed that the RSM-CCD method could efficiently be applied for the modeling of nanoparticles, which laid the foundation of the further research of immuno nanoparticles.

**Keywords:** Optimization, central composite design, response surface methodology, albumin nanoparticles, desolvation, doxorubicin

## Introduction

An experimental growth has been seen in new strategies for cancer treatment based on drug loaded nanoparticulate formulations. Nanoparticles' passive or active targeting with minor drug leakage, and good storage stability may circumvent cancer cell multidrug resistance<sup>1</sup>. Doxorubicin is one of the most effective anticancer drugs. However, its clinical usefulness is often limited by its severe adverse side effects on cardiomyopathy and congestive heart failure<sup>2,3</sup>. The toxicological study of these formulations revealed that binding of doxorubicin to the nanoparticles did not increase its acute toxicity.

Moreover, they could decrease the toxicity, given the same dose, comparing to conventional dosage forms<sup>4</sup>.

Doxorubicin has been bound to nanoparticles made of biodegradable or non-degradable materials<sup>5–8</sup>. Some of these colloidal systems reduced efficiency of transgene delivery and interactions with negatively charged molecules in serum on the cell surface, as a consequence, poor delivery to the targeted cells<sup>6,9,1</sup>. However, protein nanoparticle preparations recently seem to overcome these obstacles<sup>10–12</sup>. Especially bovine serum albumin (BSA) appears to be a suitable agent for cancer therapy, because it might avoid undesired interactions

*Address for Correspondence:* Prof. Dawei Chen, Department of Pharmaceutics, School of Pharmacy, Shenyang Pharmaceutical University, 103 Wenhua Road, Shenyang 110016, Liaoning, P. R. China. Tel.: +86 (24) 23986306. E-mail: lilei360@sina.com

(Received 08 October 2010; revised 11 February 2011; accepted 14 February 2011)

with serum that are often encountered after intravenous injection<sup>13</sup>. Albumin nanoparticles have several specific advantages: well tolerated, biodegradable, easily-prepared and reproducible. In addition, covalent linkage of nanoparticles with drug targeting ligands is possible, due to the presence of functional groups on the surfaces of the nanoparticles<sup>14–19</sup>. For this reason, the drug loading capacity of doxorubicin to albumin nanoparticles was investigated.

Basically there are three different methods of albumin nanoparticles preparation, which are based on emulsion formation, coacervation, or desolvation<sup>20–22</sup>.

The particles were prepared by the drop wise addition of ethanol to an aqueous serum albumin solution at pH values between 7 and 9, followed by glutaraldehyde cross-linking and purification by centrifugation. It was found that with the increasing pH values of albumin solution, particle size was reduced due to an increased ionization of the serum albumin (isoelectric point  $pI=5.3$ ), which leads to repulsion of the serum albumin molecules and aggregates during particle formation<sup>23,21</sup>. Research also showed that other factors, such as albumin concentrations, amount of drug, percent of glutaraldehyde and rate of dropping ethanol, also had influence on the formulation of serum albumin nanoparticles<sup>14,15,17</sup>. The current research of preparation focuses on single factor exploration, and ignores the interactions of different factors. Response surface methodology (RSM) was applied in order to explore the relationships between independent and response variables, and optimize the preparation of doxorubicin-loaded albumin nanoparticles (Dox-A-Nps).

RSM provides important information regarding the optimum level of each variable along with its interactions with other variables and their effects on product yield. It can reduce the number of experiments without neglecting the interaction among the parameters. This multivariate approach also improves statistical interpretation possibilities, and evaluates the relative significance of several affecting factors even in the presence of complex interactions. RSM is widely used for multivariable optimization studies in several biotechnological processes such as optimization of media, process conditions, catalyzed reaction conditions, oxidation, production, fermentation, bio-sorption of metals, etc<sup>24–29,43</sup>. It has also been used to determine the optimal values for process parameters such as pH value, temperature, aeration, feeding rates in various processes<sup>30–34</sup>.

The objective of the present study was to optimize the preparation of Dox-A-Nps through desolvation procedures using RSM, which showed a controllable particle diameter, good stability and high drug loading. Further investigations were focused on the influence of each variable along with its interactions with other variables on particle size, stability and drug loading, etc. using RSM in conjunction with CCD. In order to optimize Dox-A-Nps, mathematical model equations were derived by

computer simulation programming Design-Expert® version 7.0. For a better understanding of the variables for the optimal Dox-A-Nps performance, the models were presented as three-dimensional response surface graphs. The study is intended to establish a rational basis for the production and application of protein-based nanoparticles as drug carrier systems.

## Materials and methods

### Materials

BSA (fraction V, purity 96–99%) and trypsin (1:250) were obtained from Amresco Inc. (Solon, City of Solon, OH). Doxorubicin was purchased from Beijing Huafeng United Technology Co. Ltd. (Beijing, China). Coomassie brilliant blue G250 and glutaraldehyde 8% water solution were from Sigma-Aldrich Corporation (Shanghai, China). Poloxamer 188 was purchased from BASF (Ludwigshafen, Germany). Alcohol 95% and other agents were of analytical grade and used as received.

### Preparation and optimization of Dox-A-Nps

Albumin nanoparticles were prepared by using a desolvation technique. In principle, from 40 to 100 mg albumin in 1.0 ml of 10 mM NaCl solution was titrated to pH 7.5–9.5, then 1–5 mg doxorubicin was added. The mixed solutions transformed into nanoparticles in the process of continuous addition of 8.0 ml of the desolvating agent ethanol under stirring (500 rpm) at room temperature. The technique was preceded by adding a constant flow pump which enabled nanoparticles preparation at a defined rate of ethanol addition from 0.5 to 2.0 ml/min. After the desolvation process, 8% glutaraldehyde in water (between 0.235 and 1.175  $\mu\text{l}/\text{mg}$  albumin) was added to induce particle cross-linking (the amount of glutaraldehyde is equal to 40% and 200% of the calculated amount necessary for the quantitative cross-linking of the 59 amino groups in the serum albumin molecule). The cross-linking process was performed under stirring of the suspension over a time period of 24 h.

The resulting nanoparticles were purified by five cycles of differential centrifugation ( $15,000\times g$ , 5 min) and redispersion of the pellets to the original volume in 10 mM NaCl at pH values of 7.5 and 9.5, respectively. Each redispersion step was performed in an ultrasonication bath over 3 min, in order to remove the organic solvent completely.

The above albumin nanoparticle preparation procedure was optimized by a four-factor, five-level central composite design (CCD), with albumin concentration ( $X_1$ ), amount of doxorubicin ( $X_2$ ), pH ( $X_3$ ) and percentage of glutaraldehyde ( $X_4$ ) as independent variables (Table 1). Levels of those independent variables were based on preliminary trials. Mean particle size, zeta potential, drug loading, encapsulation efficiency and nanoparticles yield of the resulting Dox-A-Nps were used as response variables. Design-Expert® version 7.0 software (Stat-Ease Inc., Minneapolis, MN) was applied to generate and

Table 1. Factors and their levels in CCD designs.

Independent variables	Symbol	Coded levels				
		-1.732	-1	0	+1	+1.732
Albumin concentration (mg/ml)	X <sub>1</sub>	10	15	20	25	30
Doxorubicin amount (mg)	X <sub>2</sub>	1	2	3	4	5
pH	X <sub>3</sub>	7.5	8	8.5	9	9.5
Degree of glutaraldehyde (%)	X <sub>4</sub>	50	75	100	125	150

CCD, central composite design.

evaluate the statistical experimental design. Poloxamer 188 (1% (w/v)) was then added into the optimized Dox-A-Nps solutions in order to increase the storage stability.

### Determination of particle size and zeta potential

Mean diameter and particle size distribution were determined using a laser light scattering instrument (LS 320; Beckman, American). Zeta potential was measured using a zeta potential analyzer (Delsa 440SX; Beckman, American). The particle size and zeta potential measurements were performed in triplicate.

### Drug loading, encapsulation efficiency and nanoparticles yield

The drug loading and encapsulation efficiency of Dox-A-Nps prepared with different formulations were determined by centrifugation of the colloidal samples at 20,000×g and 12°C for 10 min, for three times. For determination of drug entrapment, the amount of drug present in the clear supernatant after centrifugation was determined by UV-spectrophotometer at 480 nm. A standard calibration curve of concentration vs. absorbance was plotted for this purpose. The amount of drug in supernatant was then subtracted from the total amount of drug added during the coacervation process. The amount of Dox entrapped within nanoparticles was calculated by the difference between the total amount used and the amount presented in the aqueous supernatant phase. The non-entrapped Dox in the supernatant obtained after ultracentrifugation of nanoparticles was determined by the method mentioned above.

Drug loading, encapsulation efficiency and nanoparticle yield were obtained from Equations (1), (2) and (3), respectively:

$$\text{Drug loading (\%)} = \frac{\text{Weight of drug in nanoparticles}}{\text{Weight of nanoparticles}} \times 100\% \quad (1)$$

$$\text{Encapsulation efficiency (\%)} = \frac{\text{Weight of drug in nanoparticles}}{\text{Weight of total drug}} \times 100\% \quad (2)$$

$$\text{Nanoparticles yield (\%)} = \frac{\text{Weight of nanoparticles recovered}}{\text{Weight of total drug and polymer}} \times 100\% \quad (3)$$

### Surface morphology

The surface morphology of the formulated nanoparticles was visualized by transmission electron microscopy (TEM). The morphology of the Dox-A-Nps was observed using a TEM (JEM-1200, JEOL Co. Ltd., Tokyo, Japan). A drop of the nanoparticles dispersion was finely spread on a copper grid coated carbon with films and negatively stained with 2% (w/v) phosphotungstic acid for viewing.

### Storage stability of optimal Dox-A-Nps

Aqueous dispersions of nanoparticles with doxorubicin embedded were stored at 4°C for a period of 120 days. After predetermined storage time points, samples were taken and the nanoparticles were redispersed in purified water. Particle size, zeta potential, drug loading and encapsulation efficiency as stability parameters were determined as described above.

### In vitro drug release study

The *in vitro* drug release profiles of Dox-A-Nps were determined as follows. About 20 mg nanoparticles were redispersed in 750 µg/ml trypsin phosphate-buffered saline (pH 7.4) and placed in a dialysis bag with a molecular cut-off of 8 kDa. Then the Dox-A-Nps contained bag was tied and put into 25 ml pre-thermostated Trypsin-PBS medium solution. The entire system was incubated at (37 ± 0.5)°C under stirring at 50 rpm. At the designated time intervals (0.5 h, 1 h, 2 h, 4 h, 6 h, 8 h, 12 h, 18 h, 24 h, 36 h, 48 h and 60 h), 2 ml of the release medium was removed and replaced with the same volume of medium solution. The amount of DOX released in the medium was determined by UV-spectrophotometry at 480 nm. All measurements were performed in triplicate.

### Data analysis

The relationships between responses and formulation variables of all model formulations were treated by Design-Expert® software. Statistical analysis including stepwise linear regression and response surface analysis was conducted. The significant terms ( $P < 0.05$ ) were chosen for final equations. Suitable models consisting of four components include linear, quadratic and special cubic models. The best fitting mathematical parameters including the coefficient ( $R^2$ ), and the adjusted multiple correlation coefficient (adjusted  $R^2$ ) proved by Design-Expert® software. Significance of differences was evalu-

ated using Student's *t*-test and one way ANOVA at the probability level of 0.05.

## Results

### Optimization of formulas

For the RSM involving CCD, a total of 30 experiments were conducted for four factors at five levels. The coded independent values and the observed responses for the 30 experiments were shown in Table 2. A suitable polynomial equation involving the main individual effects and interaction factors was selected based on the estimation of several statistical parameters provided by the Design-Expert® software. Multiple regression analysis of the experimental data yielded the following regression equation for mean particle size Equation (4), zeta potential Equation (5), drug loading Equation (6), encapsulation efficiency Equation (7) and nanoparticles yield Equation (8). All the polynomial equations were found to be statistically significant ( $P < 0.05$ ):

#### Mean particle size (nm)

$$= 364.83 - 10.75 \times X_1 + 16.08 \times X_2 - 56.08 \times X_3 + 8.75 \times X_4 + 13.63 \times X_1 \times X_2 + 18.88 \times X_1 \times X_3 + 34.50 \times X_1 \times X_4 + 57.25 \times X_2 \times X_3 + 36.1 \times X_2 \times X_4 + 11.13 \times X_3 \times X_4 + 17.58 \times X_{12-48} \cdot 54 \times X_{2^2} + 10.96 \times X_{32-36} \cdot 42 \times X_{4^2} \quad (4)$$

#### Zeta potential (mV)

$$= -7.21 + 0.69 \times X_1 - 0.45 \times X_2 - 5.1 \times X_3 + 0.92 \times X_4 + 0.84 \times X_1 \times X_2 + 0.44 \times X_1 \times X_3 + 0.48 \times X_1 \times X_4 + 0.94 \times X_2 \times X_3 + 1.25 \times X_2 \times X_4 + 1.85 \times X_3 \times X_4 - 3.3 \times X_{1^2} - 1.59 \times X_{2^2} - 0.6 \times X_{3^2} - 5.2 \times X_{4^2} \quad (5)$$

#### Drug Loading (%)

$$= 20.01 - 0.37 \times X_1 - 3.69 \times X_2 + 3.24 \times X_3 - 0.28 \times X_4 + 2.49 \times X_1 \times X_2 - 4.15 \times X_1 \times X_3 + 1.31 \times X_1 \times X_4 - 2 \times X_2 \times X_3 + 1.59 \times X_2 \times X_4 - 1.49 \times X_3 \times X_4 - 3.67 \times X_{1^2} - 2.34 \times X_{2^2} - 3.1 \times X_{3^2} - 0.56 \times X_{4^2} \quad (6)$$

#### Encapsulation efficiency (%)

$$= 77.87 + 3.3 \times X_1 + 7.63 \times X_2 + 1.7 \times X_3 + 4.35 \times X_4 - 3.80 \times X_1 \times X_2 - 2.39 \times X_1 \times X_3 - 1.59 \times X_1 \times X_4 - 2.38 \times X_2 \times X_3 - 5.27 \times X_2 \times X_4 - 0.14 \times X_3 \times X_4 - 0.37 \times X_{1^2} - 2.92 \times X_{2^2} - 1.99 \times X_{3^2} - 0.49 \times X_{4^2} \quad (7)$$

#### Nanoparticles yield (%)

$$= 82.27 + 9.01 \times X_1 - X_2 + 0.31 \times X_3 + 4.17 \times X_4 - 3.10 \times X_1 \times X_2 - 2.76 \times X_1 \times X_3 - 1.86 \times X_1 \times X_4 - 2.75 \times X_2 \times X_3 + 1.27 \times X_2 \times X_4 + 3.10 \times X_3 \times X_4 - 3.67 \times X_{1^2} - 3.73 \times X_{2^2} - 0.91 \times X_{3^2} - 1.58 \times X_{4^2} \quad (8)$$

where  $X_1$  is albumin original concentration,  $X_2$  is amount of doxorubicin,  $X_3$  is pH and  $X_4$  is percentage of glutaraldehyde.

The statistical significance of the model equation was evaluated by the *F*-test for analysis of variance (ANOVA), which showed that the regression is statistically significant at 95% ( $P < 0.05$ ) confidence level. The value of *P* less than 0.05 indicates that the model terms are also significant. The lack of fit *P*-value of  $< 0.05$  implies the lack of fit is significant. ANOVA was also applied to determine the significance and the magnitude of the effects of the main variables and their interactions on the response variables. According to the ANOVA, *P*-values for response  $Y_1$  represent that the linear contributions ( $X_3$ ), the cross product contribution ( $X_2X_3$ ) and the quadratic contribution ( $X_2^2$  and  $X_4^2$ ) are significant (Table 3). As can be seen from Figure 1, the particle size decreased markedly with the increase of pH.

The zeta potential of the Dox-A-Nps was significantly influenced by  $X_3$ ,  $X_1^2$  and  $X_4^2$  (Table 3,  $P < 0.05$ ). With increasing pH values, the zeta potential of the nanoparticles was reduced from  $-5.9$  to  $-22.0$  mV at pH values between 8 and 9 (Figure 2). As shown in Figure 2, when the albumin concentration and amount of DOX were held at center point, namely 20 mg/ml and 3 mg/ml, the zeta potential of the nanoparticles have a maximal value as the pH and percentage of glutaraldehyde arrive at 8.5 and 100%, respectively.

$X_2$ ,  $X_3$ ,  $X_1X_3$ ,  $X_1^2$  and  $X_3^2$  had a significant effect on the Dox-A-Nps on the drug loading (Table 3, Figure 3,  $P < 0.05$ ). It was obvious that the drug loading decreased with increasing pH (Figure 3). As shown in Figure 3A, with increasing pH values from 8 to 9, the drug loading of the nanoparticles was reduced from 22% to 5.5%. The drug loading increased dramatically with the decrease of amount of DOX.

In the case of entrapment efficiency ( $Y_4$ ), the factor  $X_2$ ,  $X_4$  and  $X_2X_4$  were found to be significant. As the amount of doxorubicin and percentage of glutaraldehyde increased, the entrapment efficiency also increased (Table 3, Figure 4,  $P < 0.05$ ). when the albumin concentration and pH were held at center point, namely 20 mg/ml and 8.5, encapsulation efficiency of the nanoparticles has a maximal value 81.29% as the amount of DOX and percentage of glutaraldehyde arrive at 3 mg/ml and 100%, respectively (Table 3, Figure 4,  $P < 0.05$ ).

The nanoparticles yield was found to be significantly affected by  $X_1$ ,  $X_4$ ,  $X_1^2$  and  $X_2^2$  (Table 3, Figure 5,  $P < 0.05$ ). The response surface (Figure 5) showed that with the increase of albumin concentration and percentage of glutaraldehyde, nanoparticles yield increased accordingly.

After the polynomial equations have been generated, the formulation was optimized for the responses  $Y_1$  (mean particle size (nm)),  $Y_2$  (zeta potential (mV)),  $Y_3$  (loading efficiency (%)),  $Y_4$  (drug encapsulation efficiency (%)) and  $Y_5$  (nanoparticles yield (%)). The



Table 2. Experimental design and results of the central composite design (CCD).

Preparations	Variables				Responses				
	X <sub>1</sub>	X <sub>2</sub>	X <sub>3</sub>	X <sub>4</sub>	Y <sub>1</sub>	Y <sub>2</sub>	Y <sub>3</sub>	Y <sub>4</sub>	Y <sub>5</sub>
1	15	2	8	75	645	-2.34	0	23.34	45.78
2	25	2	8	75	257	-10.23	15.13	63.46	83.93
3	15	4	8	75	268	-11.29	2.23	82.62	58.31
4	25	4	8	75	261	-10.84	2.8	79.49	72.94
5	15	2	9	75	128	-24.11	29.25	58.08	58.58
6	25	2	9	75	263	-23.83	4.51	57.67	76.02
7	15	4	9	75	356	-25.83	6.99	73.28	46.03
8	25	4	9	75	267	-28.38	6.29	80.41	65.75
9	15	2	8	125	293	-14.48	6.03	63.55	51.25
10	25	2	8	125	350	-17.46	5.00	79.59	87.29
11	15	4	8	125	296	-18.37	0.00	80.48	69.81
12	25	4	8	125	410	-17.38	19.27	77.51	78.09
13	15	2	9	125	177	-27.38	15.91	73.52	78.83
14	25	2	9	125	191	-29.38	7.41	79.14	87.04
15	15	4	9	125	362	-25.38	4.22	83.6	73.97
16	25	4	9	125	380	-23.45	5.76	83.12	81.59
17	10	3	8.5	100	467	-24.56	12.31	73.91	56.44
18	30	3	8.5	100	411	-10.38	7.06	82.51	89.52
19	20	1	8.5	100	152	-10.84	28.27	57.80	73.19
20	20	5	8.5	100	197	-10.39	1.78	78.27	72.31
21	20	3	7.5	100	585	-2.38	0.00	71.22	87.28
22	20	3	9.5	100	240	-10.94	23.95	72.24	80.76
23	20	3	8.5	50	174	-39.68	22.90	77.19	81.42
24	20	3	8.5	150	272	-10.39	21.39	78.26	81.24
25	20	3	8.5	100	350	-10.49	16.10	74.91	82.47
26	20	3	8.5	100	394	-9.38	15.97	73.93	78.85
27	20	3	8.5	100	380	-11.34	18.10	75.09	82.39
28	20	3	8.5	100	342	-8.62	22.90	80.91	83.93
29	20	3	8.5	100	347	-1.72	23.91	81.09	83.00
30	20	3	8.5	100	376	-1.72	23.10	81.29	83.00

X<sub>1</sub> is albumin concentration, X<sub>2</sub> is amount of doxorubicin, X<sub>3</sub> is pH, and X<sub>4</sub> is percentage of glutaraldehyde; Y<sub>1</sub> is mean particle size (nm), Y<sub>2</sub> is zeta potential (mV), Y<sub>3</sub> is drug loading (%), Y<sub>4</sub> is encapsulation efficiency (%), and Y<sub>5</sub> is nanoparticles yield (%).

optimum values of the variables were obtained by graphical and numerical analyses using the Design-Expert® software and based on the criterion of desirability<sup>35,36</sup>. Afterwards, a new batch of pellets with the predicted levels of formulation factors was prepared to confirm the validity of the optimization procedure. Table 4 demonstrates that the observed values of a new batch were mostly similar with predicted values within 11% of predicted error.

The optimum values of the variables were obtained by graphical and numerical analysis using the Design-Expert® software and based on the criterion of desirability<sup>37,32</sup>. The optimized formulation was achieved with 17 mg/ml albumin, 2 mg/ml DOX, pH value is 9 and 125% percentage of glutaraldehyde degree. Thus, five new batches of the Dox-A-Nps were prepared to confirm the validity of the optimization procedure. Table 4 indicates a predicted error of 11% for mean particle size, a predicted error of 6% for zeta potential (mV), a predicted error of 2.08% for loading efficiency (%), a predicted error of 1.95% for encapsulation efficiency (%) and a predicted error of 2.39% for nanoparticles yield (%).

Thereafter, all of the following experiments were conducted using Dox-A-Nps produced by this optimized formulation.

### Surface morphology of the optimized Dox-A-Nps

The TEM images of the nanoparticles revealed their spherical-like shape, as well as a range of diameters (Figure 6).

### Storage stability of the optimal Dox-A-Nps

To investigate the effect of the storage on the stability of Dox-A-Nps, Figure 7 shows the changes of particle size, zeta potential absolute value, drug loading and encapsulation efficiency against storage times for 120 days. The related properties did not change significantly.

### Drug release behavior

The drug release of Dox-A-Nps was tested for *in vitro* release in pH 7.4 (37 ± 0.5°C) PBS with 750 µg/ml trypsin added. Figure 8 displays the plot of the data expressed as the cumulative amount of DOX released from the albumin nanoparticle formulation. Free DOX exhibited

Table 3. ANOVA for the models predicted for each response.

Source	Y <sub>1</sub>			Y <sub>2</sub>			Y <sub>3</sub>			Y <sub>4</sub>			Y <sub>5</sub>		
	SS	DF	P-value	SS	DF	P-value	SS	DF	P-value	SS	DF	P-value	SS	DF	P-value
Model	3.107 × 10 <sup>5</sup>	14	0.0083**	1713.23	14	0.0482*	1750.81	14	0.0446*	3384.05	14	0.0051***	3692.76	14	0.0023**
X <sub>1</sub>	2733.50	1	0.5066	11.47	1	0.6715	3.34	1	0.7995	260.86	1	0.0528	1948.50	1	0.0001***
X <sub>2</sub>	6208.17	1	0.3248	4.87	1	0.7819	327.53	1	0.0218*	1396.85	1	0.0002***	23.98	1	0.5192
X <sub>3</sub>	75,488.17	1	0.0029**	624.95	1	0.0060**	252.06	1	0.0403*	69.42	1	0.2951	2.26	1	0.8420
X <sub>4</sub>	1837.50	1	0.5878	20.44	1	0.5721	1.83	1	0.8510	453.24	1	0.0142*	418.08	1	0.0147*
X <sub>1</sub> X <sub>2</sub>	2970.25	1	0.4921	11.24	1	0.6746	99.10	1	0.1797	231.22	1	0.0664	153.70	1	0.1155
X <sub>1</sub> X <sub>3</sub>	5700.25	1	0.3448	3.14	1	0.8239	275.07	1	0.0332*	91.22	1	0.2328	121.61	1	0.1579
X <sub>1</sub> X <sub>4</sub>	19,044.00	1	0.0948	3.66	1	0.8103	27.61	1	0.4690	40.95	1	0.4195	55.47	1	0.3314
X <sub>2</sub> X <sub>3</sub>	52,441.00	1	0.0098**	14.12	1	0.6382	63.84	1	0.2764	90.99	1	0.2333	121.17	1	0.1586
X <sub>2</sub> X <sub>4</sub>	20,880.25	1	0.0816	24.88	1	0.5337	40.58	1	0.3820	444.54	1	0.0150*	25.83	1	0.5038
X <sub>3</sub> X <sub>4</sub>	1980.25	1	0.5738	54.58	1	0.3603	35.64	1	0.4119	0.32	1	0.9419	153.57	1	0.1156
X <sub>1</sub> <sup>2</sup>	8480.19	1	0.2526	299.47	1	0.0430*	369.60	1	0.0159*	3.81	1	0.8029	369.08	1	0.0205*
X <sub>2</sub> <sup>2</sup>	64,629.76	1	0.0050**	63.39	1	0.3041	149.65	1	0.1042	233.29	1	0.0653	380.72	1	0.0189*
X <sub>3</sub> <sup>2</sup>	3293.76	1	0.4698	9.93	1	0.6929	263.30	1	0.0366*	108.91	1	0.1943	22.63	1	0.5311
X <sub>4</sub> <sup>2</sup>	36,375.05	1	0.0263*	740.39	1	0.0034**	8.47	1	0.6865	6.61	1	0.7409	68.54	1	0.2821
Residual	89,852.83	15		919.25	15		750.43	15		884.85	15		825.69	15	
Lack of fit	87,588.00	10	0.0022**	824.46	10	0.0592	682.07	10	0.0450*	821.53	10	0.0261*	810.12	10	0.0011**
Pure error	2264.83	5		94.79	5		68.37	5		63.32	5		15.57	5	
Cor total	4.006 × 10 <sup>5</sup>	29		2632.48	29		2501.24	29		4268.90	29		4518.45	29	

SS, sum of squares; DF, degree of freedom.

X<sub>1</sub> is albumin concentration, X<sub>2</sub> is amount of doxorubicin, X<sub>3</sub> is pH, X<sub>4</sub> is percentage of glutaraldehyde; Y<sub>1</sub> is mean particle size, Y<sub>2</sub> is zeta potential, Y<sub>3</sub> is drug loading, Y<sub>4</sub> is encapsulation efficiency, Y<sub>5</sub> is nanoparticles yield. \*Indicates significant at *P*-value <0.05, \*\*at *P*-value <0.01, and \*\*\*at *P*-value <0.001.

a rapid release of 100% of drug within 4 h, a complete and instantaneous release of almost the whole DOX was observed. While DOX from Dox-A-Nps were found a relative burst drug release at the initial stage and followed by a sustained release over 60 h with a cumulative amount of 84.18%.

## Discussion

The application of a factorial design as a means to optimize nanoparticles' characteristics has previously been reported<sup>38</sup>. The classical approach used in these studies, where one factor is varied whilst the others remain constant, is unlikely to reveal the possible presence of factor interactions<sup>39</sup>. Therefore, in this study the interaction of input factors with each other is emphasized, in that the effect of changing one factor will depend on the magnitude of one or more of the other factors.

The objective of the present study was to optimize the preparation procedure for Dox-A-NPs with respect to a defined particle size, zeta potential, higher drug encapsulation efficiency, loading efficiency and nanoparticles yield using RSM. Furthermore, each parameter such as the pH value, albumin concentration, amount of doxorubicin and percentage of glutaraldehyde were optimized in order to achieve a colloidal system with well-defined physicochemical characteristics.

There are three different preparation methods for drug loading of nanoparticles, based on desolvation<sup>15</sup>, coacervation<sup>40</sup>, or emulsion formation<sup>22</sup>.

In this paper, a four-factor five-level CCD as the RSM requires 30 experiments. The optimum point for Dox-A-Nps preparation was obtained by graphic method and partial derivative resolution of Equations (4–8). The most efficient condition for this preparation would use the lowest mean particle size, zeta potential, and the highest drug loading, entrapment efficiency and the nanoparticles yield. Table 4 suggested the optimum experimental condition with albumin concentration was 17 mg/ml, amount of doxorubicin was 2 mg/ml, pH value was 9 and percentage of glutaraldehyde was 125%.

Under the recommended conditions, the adequacy of the model predicted here was examined by additional independent experiments at the suggested optimal preparation conditions. The experiments were conducted in triplicate. Compared with predicted minimum mean particle size (136 nm) and zeta potential (–20 mV) which were obtained from Equations (4 and 5), the actual average value of mean particle size (151 ± 0.43 nm) and zeta potential (–18.8 ± 0.21 mV) were obtained. Compared with predicted maximum drug loading (21.4%), entrapment efficiency (76.9%) and the nanoparticles yield (82.0%) which were obtained from Equations (6–8), the actual average value of loading efficiency (20.8 ± 0.70%), entrapment efficiency (75.4 ± 0.21%) and nanoparticles yield (80.0 ± 0.34%) were obtained.

The TEM images of the nanoparticles revealed their regular spherical shape, as well as a range of diameters (Figure 6). This is much closer to the ideal particle size, which is between 100 and 200 nm. For particles larger

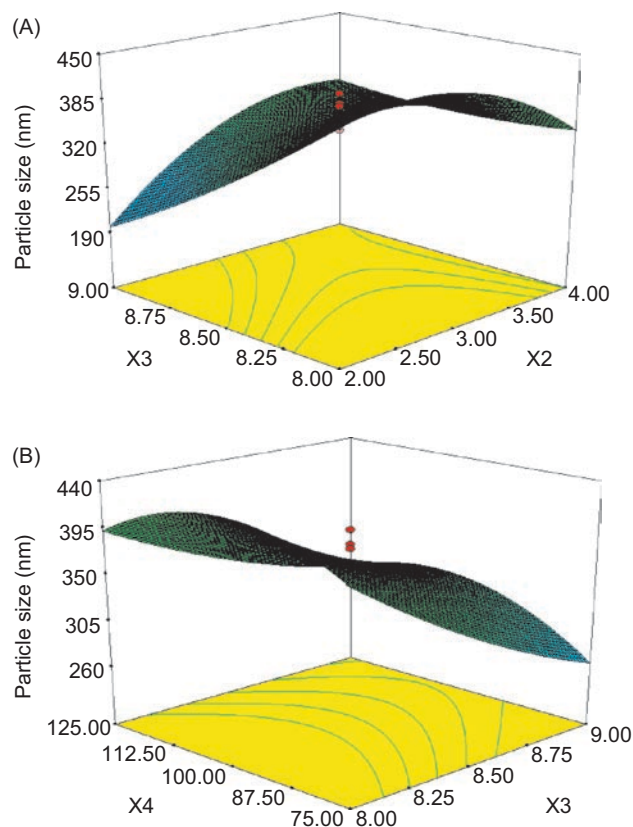


Figure 1. (A) Response surface plots for mean particle size (nm) of the Dox-A-Nps showing interaction between amount of doxorubicin and pH; (B) Response surface plots for mean particle size (nm) of the Dox-A-Nps showing interaction between percentage of glutaraldehyde and pH.

than 200 nm, the phagocytic uptake is faster because of enhanced opsonization<sup>41</sup>. Particles smaller than 100 nm are able to cross the fenestration of the hepatic sinusoidal endothelium, accumulate in the liver and have the tendency to unspecific uptake in all tissues.

Dox-A-Nps were prepared through desolvation method<sup>13</sup> because the size of Nps prepared by the method of emulsion formation and coacervation cannot be controlled easily<sup>40,22</sup>. In the earlier study, the amount of the desolvating agent ethanol in the desolvation process was found to control particle size, but the variability in size at a given ethanol amount was high in the condition of manual performance<sup>14</sup>. Considering the high variability originated from manual addition of ethanol, a constant flow pump was used, which enabled a defined rate of ethanol addition in this study.

The desolvation process determines whether albumin nanoparticles with a suitable particle size could be prepared. The pH value of the albumin solution plays an important role in the desolvation process. The isoelectric point of BSA is  $pI = 4.7$ . It indicates that the bovine serum has a positive charge below  $pI = 4.7$  and negative charge above  $pI = 4.7$ . At pH values around the  $pI$ , the nanoparticles became unstable. According to the authors' earlier research, without titrating the pH value to above 7.5, the size of the prepared was of micron grade. In aqueous

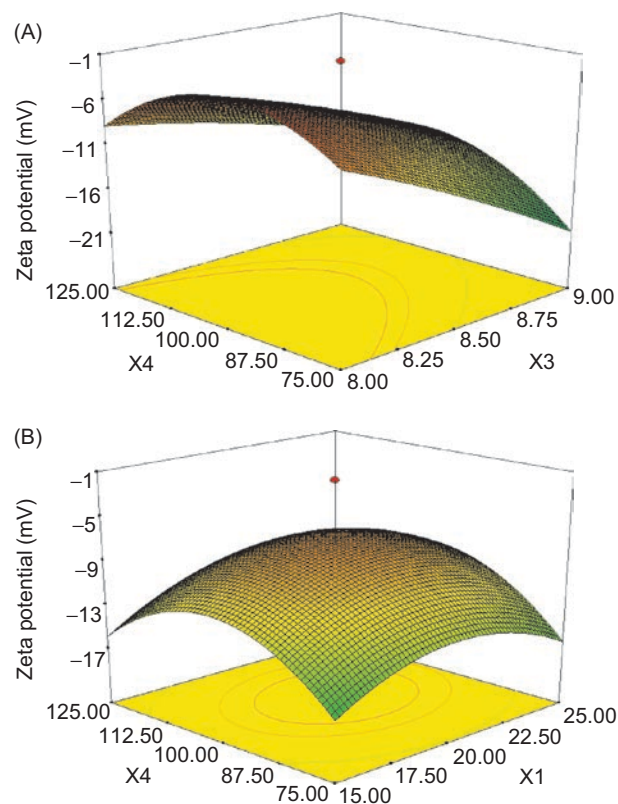


Figure 2. (A) Response surface plots for zeta potential (mV) of the Dox-A-Nps showing interaction between percentage of glutaraldehyde and pH; (B) Response surface plots for zeta potential (mV) of the Dox-A-Nps showing interaction between albumin concentration and percentage of glutaraldehyde.

media, the pH of the sample is one of the most important factors that affect its zeta potential. If more alkali is added to the particles suspension with a negative zeta potential, the particles tend to acquire more negative charge. Maybe it's the reason why increasing pH values led to the increase of zeta potential absolute value.

For the purpose of increasing the zeta potential and stability of the prepared nanoparticles, 10 mM NaCl solution instead of water, was employed as the solvent of albumin, which could increase the ion concentration and electric conductivity of the solution.

The zeta potential absolute value of the optimized nanoparticles without adding Poloxamer 188 showed a decrease of 10 mV from 24 mV to 14 mV from 1 week to 6 weeks time duration, which indicated the stability was still to be improved. In order to increase the stability of the optimized Dox-A-Nps, Poloxamer 188 was chosen as stabilizer. The zeta potential decreased with surfactant because Poloxamer 188 had the typical characteristics of surfactant which could decrease the surface tension between the particles and the solution. As a result, the addition of Poloxamer 188 led to the decrease of zeta potential, which could strengthen the stability dramatically.

According to the *in vitro* results (Figure 8), two stages appeared in the release curve of Dox from albumin nanoparticles. The first one was a burst effect from 0.5 to 8 h,



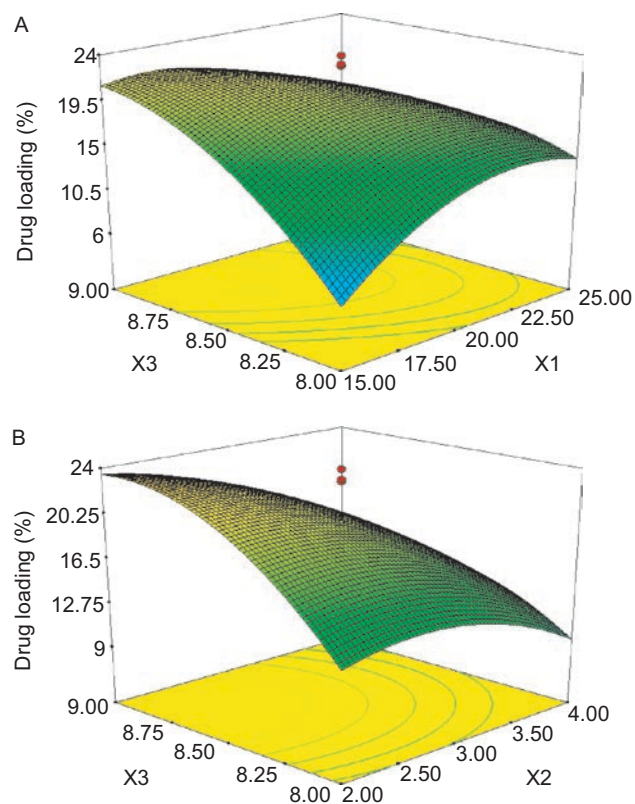


Figure 3. (A) Response surface plots for amount of drug loading (%) of the Dox-A-Nps showing interaction between albumin concentration and pH; (B) Response surface plots for amount of drug loading (%) of the Dox-A-Nps showing interaction between amount of doxorubicin and pH.

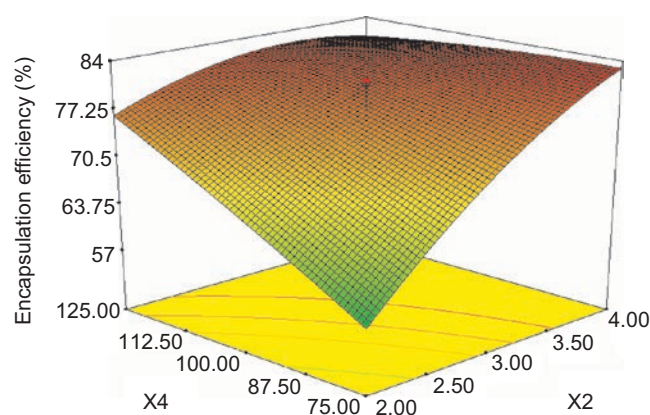


Figure 4. Response surface plots for encapsulation efficiency (%) of the Dox-A-Nps showing interaction between amount of doxorubicin and percentage of glutaraldehyde.

and the second one was a sustained release from 8 to 60 h with a cumulative amount of 84.18%. This indicated the ways of drug loading in the albumin nanoparticles: adsorption and entrapment. The results of the curve fitting indicated that the drug release from the albumin nanoparticles in the presence of trypsin could be described as an erosion sphere model<sup>42,43</sup> (Heison and Crowell cube-root equation).

Particle size is a crucial parameter, in particular for the *in vivo* behavior of nanoparticles after intravenous injection<sup>15</sup>. In order to influence the resulting particle size, we studied the linear, square, and interactive effects of the albumin concentration, amount of Dox, pH value of the protein solution and percentage of glutaraldehyde.

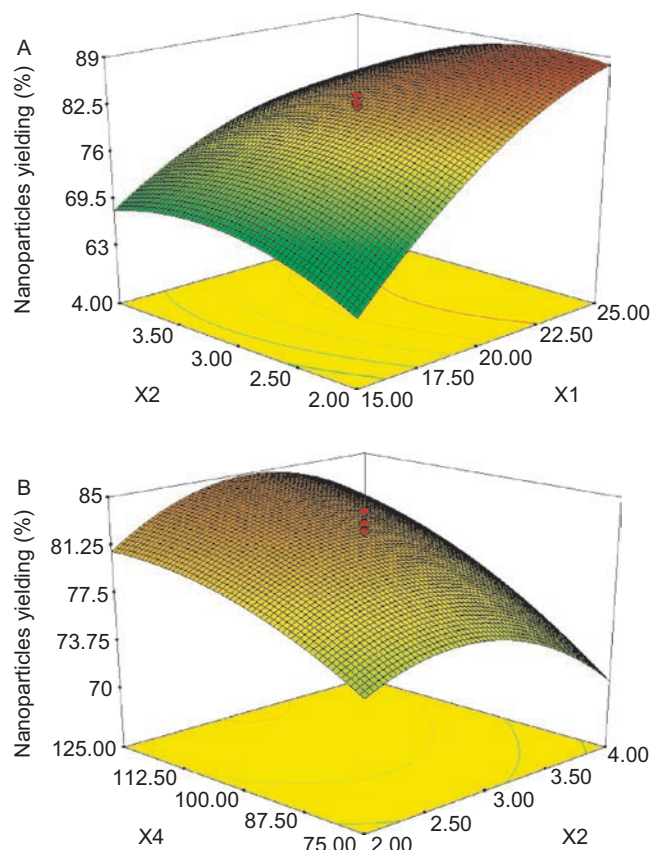


Figure 5. (A) Response surface plots for nanoparticles yielding (%) of the Dox-A-Nps showing interaction between albumin concentration and amount of doxorubicin; (B) Response surface plots for nanoparticles yielding (%) of the Dox-A-Nps showing interaction between amount of doxorubicin and percentage of glutaraldehyde.

Table 4. Optimized formulation of the Dox-A-Nps and the predicted and observed responses.

Factors		Predicted response		Observed responses		Predicted error (%)
X <sub>1</sub>	17 mg/ml	Y <sub>1</sub>	136 nm	Y <sub>1</sub>	151 ± 0.43 nm	11.0
X <sub>2</sub>	2 mg/ml	Y <sub>2</sub>	-20 mV	Y <sub>2</sub>	-18.8 ± 0.21 mV	6.00
X <sub>3</sub>	9	Y <sub>3</sub>	21.4%	Y <sub>3</sub>	20.8 ± 0.70%	2.08
X <sub>4</sub>	125%	Y <sub>4</sub>	76.9%	Y <sub>4</sub>	75.4 ± 0.21%	1.95
		Y <sub>5</sub>	82.0%	Y <sub>5</sub>	80.0 ± 0.34%	2.39

X<sub>1</sub> is albumin concentration, X<sub>2</sub> is amount of doxorubicin, X<sub>3</sub> is pH, X<sub>4</sub> is percentage of glutaraldehyde, Y<sub>1</sub> is mean particle size (nm), Y<sub>2</sub> is zeta potential (mV), Y<sub>3</sub> is drug loading (%), Y<sub>4</sub> is encapsulation efficiency (%), Y<sub>5</sub> is nanoparticles yield (%).



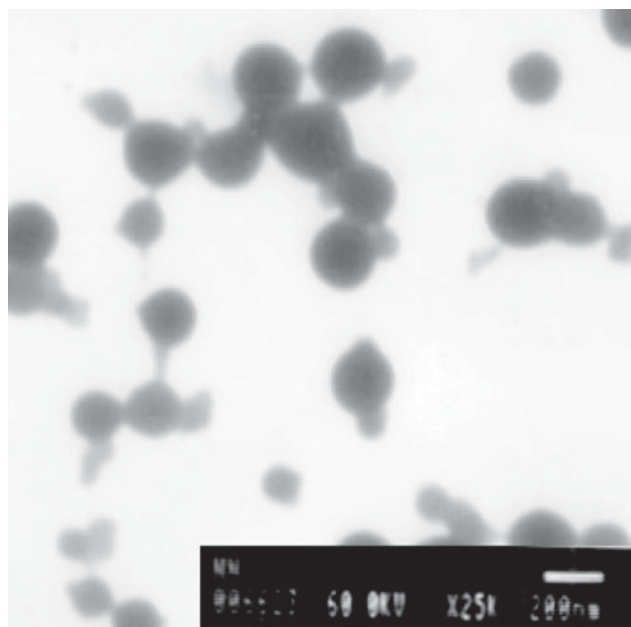


Figure 6. Transmission Electron Microphotographs of optimized doxorubicin-loaded albumin nanoparticles.

This study shows that pH, the square of amount of DOX, percentage of glutaraldehyde and the interactive pH and amount of DOX influence the desolvation in the process of nanoparticles preparation. The doxorubicin, which was used in the experiments, dissociates in water into the protonized anthracycline and negatively charged chloride ions. Ionic compounds such as salts were previously shown to influence the particle formation. Both observations are in good agreement with the earlier work of Langer K who found that the pH value of the HSA solution prior to the desolvation procedure was identified as the major factor determining particle size. Higher pH values leading to smaller nanoparticles. The effect of glutaraldehyde, which was used for cross-linking of the nanoparticles, on size of particle was investigated. There was no influential concentration to have any impact on particle size (Table 3, Figure 1). A similar result was declared on fabrication of protein nanoparticles using human serum albumin. Langer<sup>15</sup> reported that glutaraldehyde concentrations had no influence on particle size.

Zeta potential is significantly affected by pH, the square of albumin concentration and percentage of glutaraldehyde (Table 3, Figure 2). In the desolvation process, higher zeta potential is associated with high stability of the colloidal system. We can say that the relative albumin concentration, pH and percentage of glutaraldehyde play significant roles in determining the over-all electrical properties of the nanoparticles. That parameter of the effect of drug content on the size and stability of nanoparticles has not been addressed in the present literature.

Drug loading, entrapment efficiency and nanoparticles yield are important aspects in the production of Dox-A-Nps. The preparation procedure must return a useful yield of nanoparticles, particularly if their

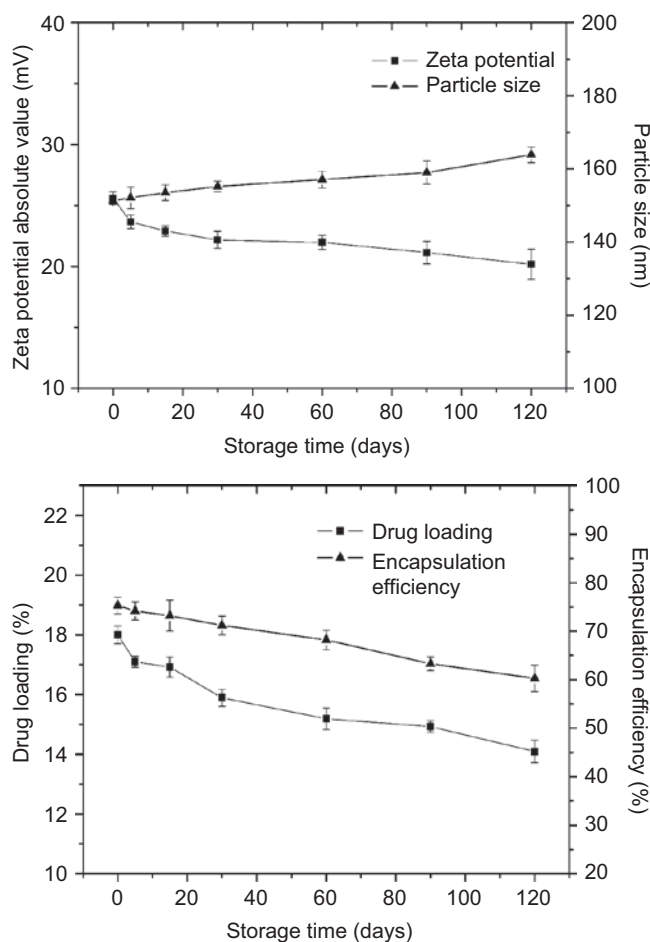


Figure 7. The mean particle size, zeta potential, drug loading and encapsulation efficiency of Dox-A-Nps against storage time at 4°C.

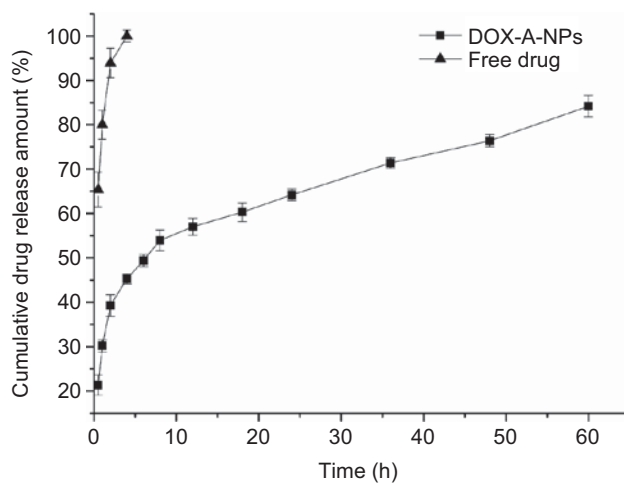


Figure 8. *In vitro* drug release profiles of DOX from albumin and free drug ( $n=3$ ).

intended DOX-loading is an expensive material to produce. If the process is not optimized, large, amorphous, polymeric flakes are produced. This is both wasteful in terms of DOX consumption and loss of incorporated DOX. Using ANOVA, it was shown that pH, pH<sup>2</sup>, albumin concentration<sup>2</sup> and the interactions of the pH value and albumin concentration have a strong influence on

loading efficiency, whereas the amount of DOX and glutaraldehyde used play a minor role. Thus, it is possible to use low levels of these two factors, reducing wastage of DOX; whereas, the percentage of glutaraldehyde, the interaction of the amount of DOX rate and percentage of glutaraldehyde had a significant effect on the Dox-A-Nps on the entrapment efficiency. The albumin concentration, percentage of glutaraldehyde, albumin concentration<sup>2</sup> and DOX<sup>2</sup> had a significant effect on the Dox-A-Nps on the nanoparticles yield. (Table 3, Figure 4,  $P < 0.05$ ).

## Conclusion

A desolvation method was employed to prepare the Dox-A-Nps. The Dox-A-Nps was optimized using the CCD-RSM by fitting a second-order model to the response data. The optimum experimental condition was as follows, albumin concentration was 17 mg/ml, amount of doxorubicin was 2 mg/ml, pH value was 9 and percentage of glutaraldehyde was 125%. The experimental values of the Dox-A-Nps prepared under the optimum conditions were mostly close to the predicted ones.

In conclusion, these results showed that the generated model adequately predicted the percent drug loading capacity and controlled drug release. RSM was an efficient tool being used in the process of optimizing the preparation of albumin nanoparticles.

## Declaration of interest

The manuscript has been submitted solely to this journal and is not published, in press, or submitted elsewhere. All the research meets the ethical guidelines, including adherence to the legal requirements of the study country. The authors report no declarations of interest.

## References

- Choi K, Wang X, Nie S, Chen ZG, Shin DM. (2008). Therapeutic nanoparticles for drug delivery in cancer. *Clin Cancer Res*, 14:1310-1316.
- Singal PK, Li T, Kumar D, Danelisen I, Iliskovic N. (2000). Adriamycin-induced heart failure: mechanism and modulation. *Mol Cell Biochem*, 207:77-86.
- Minotti G, Menna P, Salvatorelli E, Cairo G, Gianni L. (2004). Anthracyclines: molecular advances and pharmacologic developments in antitumor activity and cardiotoxicity. *Pharmacol Rev*, 56:185-229.
- Gelperina SE, Khalansky AS, Skidan IN, Smirnova ZS, Bobruskin AI, Severin SE et al. (2002). Toxicological studies of doxorubicin bound to polysorbate 80-coated poly(butyl cyanoacrylate) nanoparticles in healthy rats and rats with intracranial glioblastoma. *Toxicol Lett*, 126:131-141.
- Steiniger SC, Kreuter J, Khalansky AS, Skidan IN, Bobruskin AI, Smirnova ZS et al. (2004). Chemotherapy of glioblastoma in rats using doxorubicin-loaded nanoparticles. *Int J Cancer*, 109:759-767.
- Cuvier C, Roblot-Treupel L, Millot JM, Lizard G, Chevillard S, Manfait M et al. (1992). Doxorubicin-loaded nanospheres bypass tumor cell multidrug resistance. *Biochem Pharmacol*, 44:509-517.
- Leo E, Cameroni R, Forni F. (1999). Dynamic dialysis for the drug release evaluation from doxorubicin-gelatin nanoparticle conjugates. *Int J Pharm*, 180:23-30.
- Yoo HS, Oh JE, Lee KH, Park TG. (1999). Biodegradable nanoparticles containing doxorubicin-PLGA conjugate for sustained release. *Pharm Res*, 16:1114-1118.
- Plank C, Mechtler K, Szoka FC, Wagner E. (1996). Activation of the complement system by synthetic DNA complexes: A potential barrier for intravenous gene delivery. *Human Gene Ther*, 7:1437-1446.
- Orson FM, Kinsey BM, Hua PJ, Bhogal BS, Densmore CL, Barry MA. (2000). Genetic immunization with lung-targeting macroaggregated polyethyleneimine-albumin conjugates elicits combined systemic and mucosal immune responses. *J Immunol*, 164:6313-6321.
- Orson FM, Song L, Gautam A, Densmore CL, Bhogal BS, Kinsey BM. (2002). Gene delivery to the lung using protein/polyethylenimine/plasmid complexes. *Gene Ther*, 9:463-471.
- Truong-Le VL, Walsh SM, Schweibert E, Mao HQ, Guggino WB, August JT et al. (1999). Gene transfer by DNA-gelatin nanospheres. *Arch Biochem Biophys*, 361:47-56.
- Simões S, Slepishkin V, Pires P, Gaspar R, Pedrosa de Lima MC, Düzgünes N. (2000). Human serum albumin enhances DNA transfection by lipoplexes and confers resistance to inhibition by serum. *Biochim Biophys Acta*, 1463:459-469.
- Weber C, Coester C, Kreuter J, Langer K. (2000). Desolvation process and surface characterisation of protein nanoparticles. *Int J Pharm*, 194:91-102.
- Langer K, Balthasar S, Vogel V, Dinauer N, von Briesen H, Schubert D. (2003). Optimization of the preparation process for human serum albumin (HSA) nanoparticles. *Int J Pharm*, 257:169-180.
- Nobs L, Buchegger F, Gurny R, Allemann E. (2004). Current methods for attaching targeting ligands to liposomes and nanoparticles. *J Pharm Sci*, 93:1980-1992.
- Wardick H, Michaelis K, Balthasar S, Strebhardt K, Kreuter J, Langer K. (2004). Highly specific HER2-mediated cellular uptake of antibody-modified nanoparticles in tumour cells. *J Drug Target*, 12:461-471.
- Dinauer N, Balthasar S, Weber C, Kreuter J, Langer K, von Briesen H. (2005). Selective targeting of antibody-conjugated nanoparticles to leukemic cells and primary T-lymphocytes. *Biomaterials*, 26:5898-5906.
- Steinhauser I, Spänkuch B, Strebhardt K, Langer K. (2006). Trastuzumab-modified nanoparticles: optimisation of preparation and uptake in cancer cells. *Biomaterials*, 27:4975-4983.
- Gallo JM, Hung CT, Perrier DG. (1984). Analysis of albumin microsphere preparation. *Int J Pharm*, 22:63-74.
- Lin W, Coombes AG, Davies MC, Davis SS, Illum L. (1993). Preparation of sub-100 nm human serum albumin nanospheres using a pH-coacervation method. *J Drug Target*, 1:237-243.
- Müller BG, Leuenberger H, Kissel T. (1996). Albumin nanospheres as carriers for passive drug targeting: an optimized manufacturing technique. *Pharm Res*, 13:32-37.
- Westcott CC. (1978). *pH Measurements*. New York, USA: Academic Press.
- Kristo E, Biliaderis CG, Tzanetakis N. (2003). Modeling of the acidification process and rheological properties of milk fermented with a yogurt starter culture using response surface methodology. *Food Chem*, 83:437-446.
- Beg QK, Saxena RK, Gupta R. (2002). Kinetic constants determination for an alkaline protease from *Bacillus mojavensis* using response surface methodology. *Biotechnol Bioeng*, 78:289-295.
- Lai LST, Pan CC, Tzeng BK. (2003). The influence of medium design on lovastatin production and pellet formation with a high-producing mutant of *Aspergillus terreus* in submerged cultures. *Process Biochem*, 38:1317-1326.
- Soo EL, Salieh AB, Basri M. (2004). Response surface methodological study on lipase-catalyzed synthesis of amino acid surfactants. *Process Biochem*, 39:1151-1158.

28. Wang YX, Lu ZX. (2005). Optimization of processing parameters for the mycelial growth and extracellular polysaccharide production by *Boletus* spp. ACCC 50328. *Process Biochem*, 40:1043–1051.
29. Preetha B, Viruthagiri T. (2007). Application of response surface methodology for the biosorption of copper using *Rhizopus arrhizus*. *J Hazard Mater*, 143:506–510.
30. Mannan S, Fakhrul-Razi A, Alam MZ. (2007). Optimization of process parameters for the bioconversion of activated sludge by *Penicillium corylophilum*, using response surface methodology. *J Environ Sci (China)*, 19:23–28.
31. Chang JS, Tsai YH, Wu PC, Huang YB. (2007). The effect of mixed-solvent and terpenes on percutaneous absorption of meloxicam gel. *Drug Dev Ind Pharm*, 33:984–989.
32. Pan CM, Fan YT, Xing Y, Hou HW, Zhang ML. (2008). Statistical optimization of process parameters on biohydrogen production from glucose by *Clostridium* sp. *Fanp2. Bioresour Technol*, 99:3146–3154.
33. Shah SN, Asghar S, Choudhry MA, Akash MS, ur Rehman N, Baksh S. (2009). Formulation and evaluation of natural gum-based sustained release matrix tablets of flurbiprofen using response surface methodology. *Drug Dev Ind Pharm*, 35:1470–1478.
34. Liu CH, Wu CT, Fang JY. (2010). Characterization and formulation optimization of solid lipid nanoparticles in vitamin K1 delivery. *Drug Dev Ind Pharm*, 36:751–761.
35. Kim MS, Kim JS, You YH, Park HJ, Lee S, Park JS et al. (2007). Development and optimization of a novel oral controlled delivery system for tamsulosin hydrochloride using response surface methodology. *Int J Pharm*, 341:97–104.
36. Myers RH, Montgomery DC. (2002). *Response Surface Methodology*, 2nd Edition. New York, USA: John Wiley & Sons.
37. Harris PL, Cuppett SL, Bullerman LB. (1990). Optimization of lipase synthesis by *Pseudomonas fluorescens* by response surface methodology. *J Food Protect*, 53:481–483.
38. Lescure F, Zimmer C, Roy R, Couveur P. (1992). Optimization of poly(alkylcyanoacrylate) nanoparticles: influence of sulphur dioxide and pH on nanoparticles characteristics. *J Colloid Interf Sci*, 154:77–86.
39. Armstrong NA, James KC. (1990). *Understanding Experimental Design and Interpretation in Pharmaceuticals*. Ellis Horwood, Chichester, UK.
40. Lin W, Garnett MC, Davis SS, Schacht E, Ferruti P, Illum L. (2001). Preparation and characterisation of rose Bengal-loaded surface-modified albumin nanoparticles. *J Control Release*, 71:117–126.
41. Haley B, Frenkel E. (2008). Nanoparticles for drug delivery in cancer treatment. *Urol Oncol*, 26:57–64.
42. Sun JX, Wang LN, Yin L, Zhang ZX. (2004). Determination of 10-hydroxycamptothecin in tissues of rats by HPLC-FD. *J China Pharm Univ*, 35:540–544.
43. Vergnaud JM. (1993). *Controlled Drug Release of Oral Dosage Forms*. Chichester, UK: Ellis Horwood.
44. Dhiman MK, Yedurkar PD, Sawant KK. (2008). Buccal bioadhesive delivery system of 5-fluorouracil: optimization and characterization. *Drug Dev Ind Pharm*, 34:761–770.